0026-895X/86/040331-16$02.00/0

MOLECULAR PHARMACOLOGY, 29:331–346

Characterization of the A_2 Adenosine Receptor Labeled by [^{3}H]NECA in Rat Striatal Membranes

ROBERT F. BRUNS, GINA H. LU, and THOMAS A. PUGSLEY

Department of Pharmacology, Warner-Lambert/Parke-Davis Pharmaceutical Research, Ann Arbor, Michigan 48105

Received June 17, 1985; Accepted January 13, 1986

SUMMARY

[^{3}H]NECA (1-(6-amino-9H-purin-9-yl)-1-deoxy-*N*-ethyl-β-D-ribofuronamide) is known to bind to both the A_1 and A_2 subtypes of adenosine receptor in rat striatal membranes. In order to study the putative A_2 component of [^{3}H]NECA binding, we examined several compounds for the ability to selectively eliminate the A_1 component of binding; N^6-cyclopentyladenosine was found to give the most satisfactory results. Binding of [^{3}H]NECA in the presence of 50 nM N^6-cyclopentyladenosine was characterized. The rank order of potency for inhibition of [^{3}H]NECA binding was NECA ≫ 2-chloroadenosine > N^6-[(*R*)-1-methyl-2-phenylethyl]adenosine (*R*-PIA) > N^6-cyclohexyladenosine > *S*-PIA, indicating that binding was to an A_2 adenosine receptor. When affinities of compounds in [^{3}H]NECA binding to A_2 receptors were compared to their affinities in [^{3}H]N^6-cyclohexyladenosine binding to A_1 receptors, N^6-cyclopentyladenosine was the most A_1-sensitive agonist (A_1 K_i, 0.59 nM; A_2 K_i, 460 nM; K_i ratio, 780), whereas the selective coronary vasodilator 2-(phenylamino)adenosine was the most A_2-selective agonist (A_1, 560 nM; A_2, 120 nM; ratio, 0.21). The antagonist 8-cyclopentyltheophylline had considerable A_1 selectivity (A_1, 11 nM; A_2, 1400 nM; ratio, 130), whereas alloxazine had slight A_2 selectivity (A_1, 5200 nM; A_2, 2700; ratio, 0.52). [^{3}H]NECA binding to A_2 receptors was highest in striatum but was detectable at much lower levels in each of seven other brain areas. The regional distribution of [^{3}H]NECA binding and the affinities of adenosine agonists and antagonists for inhibition of binding indicate that the site labeled by [^{3}H]NECA belongs to the high affinity, or A_{2a}, subclass of A_2 receptor.

Extracellular adenosine receptors have been divided into two major subclasses: A_1 receptors which mediate inhibition of adenylate cyclase, and A_2 receptors which mediate stimulation of the enzyme (1). These are called R_i and R_a, respectively, in an alternate nomenclature (2). In addition to having opposite effects on generation of cyclic AMP, A_1 and A_2 receptors differ in their sensitivity to adenosine agonists. According to the "classical" description of A_1 and A_2 receptors, adenosine itself has nanomolar affinity for A_1 receptors but micromolar affinity for A_2 receptors (1, 3). At A_1 receptors, *R*-PIA[1] (Fig. 1) is more potent than NECA, whereas at A_2 receptors the reverse holds (2).

Daly *et al.* (4) further refined adenosine receptor taxonomy by dividing A_2 receptors into two classes, based upon the observation (5, 6) that some A_2 receptors have EC_{50} values for adenosine in the high nanomolar range (i.e., 10^{-7}–10^{-6} M) rather than in the micromolar range. The high affinity A_2 receptors exist in the striatum and nucleus accumbens and can be observed in broken cell adenylate cyclase assays (6), whereas the low affinity receptor exists in almost all areas of the brain and can be observed in studies of cyclic AMP accumulation in brain slices, but not in broken cell adenylate cyclase preparations.

Receptor-binding studies at A_1 receptors have been performed using the agonist radioligands [^{3}H]CHA (7), [^{3}H]*R*-PIA (8), and [^{3}H]2-chloroadenosine (9, 10), and the antagonist [^{3}H]DPX (7). A_1 receptor binding has been demonstrated in brain (7–9), testes (1), fat cells (12), and heart (13).

Although attempts to label A_2 receptors with several different radioligands have been reported, most of these have not been completely successful. [^{3}H]DPX labeled two sites in guinea pig brain membranes: an A_1 receptor with a high affinity for CHA, and a second site with a much lower affinity for CHA (7). Although the second site was initially thought to be an A_2 receptor, a structure-activity analysis indicated that most of this binding was not to adenosine receptors (7). In a short communication (14), [^{3}H]2-chloroadenosine binding in human placental membranes was found to have A_2-like properties; a

[1] *R*-PIA is equivalent to L-PIA, *l*-PIA, and (−)-PIA and is the product of the reaction of *l*-amphetamine with 6-chloro-9-β-D-ribofuranosylpurine. *S*-PIA is equivalent to D-PIA, *d*-PIA, and (+)-PIA and is the product of the reaction of *d*-amphetamine with 6-chloro-9-β-D-ribofuranosylpurine. The Cahn-Ingold-Prelog (*R*,*S*) nomenclature is preferred, since it allows the direct derivation of the absolute configurations of the PIA diastereomers.

ABBREVIATIONS: CHA, N^6-cyclohexyladenosine; CPA, N^6-cyclopentyladenosine; CPT, 8-cyclopentyltheophylline; CV-1674, 2-(4-methoxyphenyl)adenosine; CV-1808, 2-(phenylamino)adenosine; DPX, 1,3-diethyl-8-phenylxanthine; NECA, 5′-*N*-ethylcarboxamide-adenosine (systemic name: 1-(6-amino-9H-purin-9-yl)-1-deoxy-*N*-ethyl-β-D-ribofuronamide); *R*-PIA, N^6-[(*R*)-1-methyl-2-phenylethyl]adenosine; PD 113,297, 8-{4-[*N*-(3-dimethylaminopropyl)sulfonamido]phenyl}-1,3-dipropylxanthine; *S*-PIA, N^6-[(*S*)-1-methyl-2-phenylethyl]adenosine; SAR, structure-activity relationship.

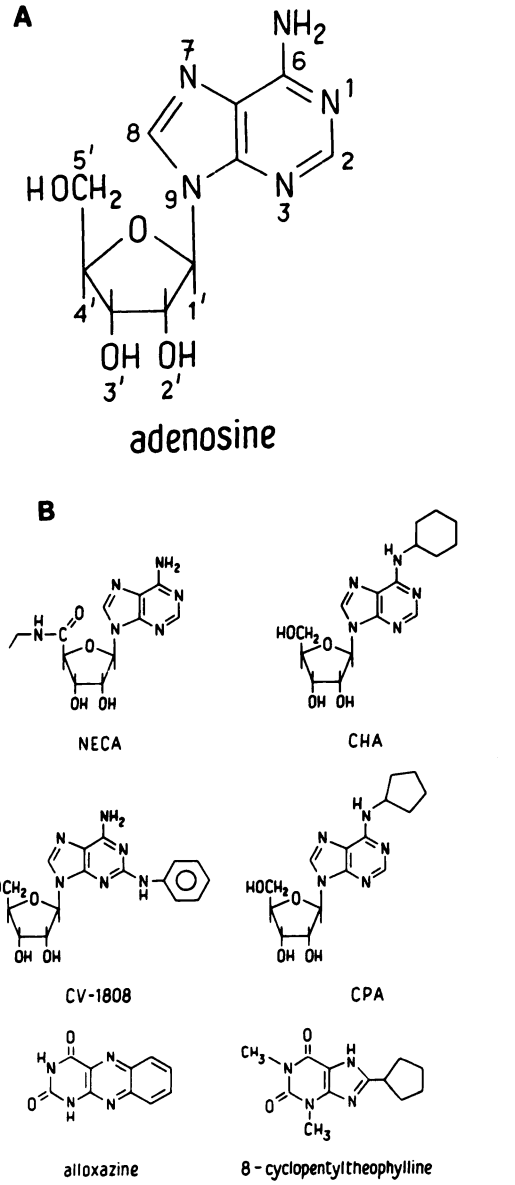

Fig. 1. Structures.

more detailed structure-activity analysis will be necessary to definitively identify these sites as A_2 adenosine receptors.

The high affinity of NECA for A_2 receptors has inspired a number of attempts to label A_2 receptors with [^{3}H]NECA. In human platelet membranes, [^{3}H]NECA bound with moderately high affinity (15). The [^{3}H]NECA binding, however, had a low affinity for theophylline (IC_{50} 800 μM) and could not be inhibited by *R*-PIA; these results are not consistent with known properties of A_1 and A_2 adenosine receptors. [^{3}H]NECA binding in liver membranes also lacked the characteristics expected of an adenosine receptor (16). In an autoradiographic study in guinea pig intestine, the potent adenosine antagonist 8-phenyltheophylline (17, 18) did not compete with [^{3}H]NECA (19).

In contrast to the above studies, Yeung and Green (20) found that [^{3}H]NECA bound to sites with the characteristics of true adenosine receptors in rat striatal membranes. Dose-inhibition curves for CHA and *R*-PIA were biphasic, suggesting that the ligand was binding to both A_1 and A_2 receptors. The A_1 component of binding could be at least partially eliminated by pretreatment of the membranes with the sulfhydryl alkylating agent *N*-ethylmaleimide. Limited structure-activity studies on the remaining sites provided results which were consistent with an A_2 adenosine receptor.

In the present study, we demonstrate that CPA can be utilized to selectively eliminate the A_1 component of [^{3}H]NECA binding to rat striatal membranes without the use of covalent protein-modifying reagents. [^{3}H]NECA binding in the presence of 50 nM CPA has the characteristics of a high affinity A_2 adenosine receptor. Using this assay in conjunction with the A_1 assay (7), we have been able to identify compounds with selectivity for A_1 or A_2 receptors. A preliminary account of these results has been published (21).

Experimental Procedures

Materials. [^{3}H]NECA was from Amersham (specific activity 27 Ci/mmol) or New England Nuclear (specific activity 30 Ci/mmol). [^{3}H]NECA from both sources gave essentially the same results. [^{3}H]CHA was from New England Nuclear (specific activity 25 Ci/mmol). Adenosine deaminase was Sigma type III, Tris·HCl was Sigma pH 7.7 preset crystals, GF/B filters were from Whatman, Formula 947 was from New England Nuclear, and CPA was synthesized by Dr. Walter Moos at Warner-Lambert/Parke-Davis. Pentostatin (2′-deoxycoformycin) was from Warner-Lambert/Parke-Davis.

Tissue preparation for [^{3}H]NECA binding. Brains from 200–500-g mixed sex Sprague-Dawley rats were purchased from Pel-Freez. Fresh brains from male Long-Evans hooded rats (Blue Spruce Farms) gave essentially identical results. Brains were thawed and then kept on ice while the striata were dissected out. Striata were disrupted in 10 volumes of ice-cold 50 mM Tris·HCl (pH 7.7 at 25°, pH 8.26 at 5°) (Tris) for 30 sec with a Polytron PT-10 homogenizer (Brinkmann) at setting 5. The suspension was centrifuged at 50,000 × *g* for 10 min, the supernatant was discarded, and the pellet was resuspended with a Polytron in 10 volumes of ice-cold Tris as above, recentrifuged, resuspended at 1 *g*/5 ml, and stored in plastic vials at −70° (stable for at least 6 months). When needed, tissue was thawed at room temperature, disrupted in a Polytron, and kept on ice until used.

Incubation conditions for [^{3}H]NECA binding. All incubations were in triplicate for 60 min at 25° in 12 × 75-mm glass tubes containing 1 ml of Tris with 5 mg of original tissue weight of rat striatal membranes, 4 nM [^{3}H]NECA, 50 nM CPA (to eliminate A_1 receptor binding), 10 mM $MgCl_2$, 0.1 unit/ml of adenosine deaminase (calculated from manufacturer's specifications), and 1% dimethylsulfoxide. CPA was omitted from those experiments where both the A_1 and A_2 components of binding were studied. The order of incubations was randomized for all experiments except time course studies and routine IC_{50} determinations. CPA was dissolved at 10 mM in dimethylsulfoxide and diluted to 500 nM in Tris on the day of the experiment. Test compounds for competition studies were dissolved at 10 mM in dimethylsulfoxide on the same day as the experiment and diluted in dimethylsulfoxide to 100 times the final incubation concentration. Control incubations received an equal volume (10 μl) of dimethylsulfoxide; the resulting concentration of dimethylsulfoxide had no effect on specific binding. [^{3}H]NECA was diluted to 40 nM in Tris. The membrane suspension (5 mg/0.79 ml) contained sufficient $MgCl_2$ and adenosine deaminase to give 10 mM and 0.1 unit/ml, respectively, final concentration in the incubation. For test compounds with IC_{50} values less than 1 μM, the order of additions was test compound (10 μl), CPA (100 μl), [^{3}H]NECA (100 μl), and membranes (0.79 ml). For test compounds with IC_{50} values greater than 1 μM and limited water solubility, the order of additions (same volumes) was test compound, membranes, CPA, and [^{3}H]NECA. After all additions, the rack of tubes was vortexed, and the tubes were then incubated for 60 min at 25° in a shaking water bath. The rack of tubes was vortexed an additional time halfway through the incubation.

Incubations were terminated by filtration through 2.4-cm GF/B

filters under reduced pressure. Each tube was filtered as follows: the contents of the tube were poured onto the filter, 4 ml of ice-cold Tris were added to the tube and the contents poured onto the filter, and the filter was washed twice with 4 ml of ice-cold Tris. The filtration was complete in about 12 sec. In some experiments, the samples were filtered with a Brandel 48R cell harvester through a GF/B filter sheet. In this case, the tubes were washed three times with 3 ml of ice-cold Tris. The damp filters were put in scintillation vials, 8 ml of Formula 947 scintillation fluid were added, and the vials were left overnight, shaken, and counted in a liquid scintillation counter at 40% efficiency. Recovery of radioactivity was lower if filters were allowed to dry out before addition of scintillation fluid.

[^{3}H]CHA binding. [^{3}H]CHA binding to A_1 receptors (7) was performed using the same protocol as [^{3}H]NECA binding with the following exceptions: the radioligand was 1 nM [^{3}H]CHA, the tissue was 20 mg of whole rat brain (minus cerebellum and brainstem) from male Long-Evans hooded rats, the 10 mM $MgCl_2$ and 50 nM CPA were omitted, and the volume was 2 ml.

Data analysis. Nonspecific binding of [^{3}H]NECA was defined as binding in the presence of 100 μM CPA. For [^{3}H]CHA, 1 mM theophylline was used for nonspecific binding. Specific binding was defined as total binding minus nonspecific binding. IC_{50} values were calculated by weighted nonlinear least squares curve fitting to the mass-action (Langmuir) equation:

$$Y = T - S \cdot \frac{D}{D + K}$$

where Y is cpm bound, T is cpm total binding without drug, S is cpm specific binding without drug, D is the concentration of drug, and K is the IC_{50} of the drug. Weighting factors were calculated under the assumption that the standard deviation was proportional to the predicted value of Y. Nonspecific binding was treated as a very large (infinite) concentration of drug in the computer calculation of IC_{50} values.

A_1 K_i values were calculated by the following procedure. Since [^{3}H]CHA binds to two or more sites of different affinities (22), an average K_d of 1.31 nM for the sites occupied by 1 nM [^{3}H]CHA was calculated from the IC_{50} (2.31 nM) for unlabeled CHA versus 1 nM [^{3}H]CHA by the equation:

$$K_d = IC_{50} - L$$

where L is the ^{3}H-ligand concentration. IC_{50} values for compounds were then converted to K_i values by multiplying by 0.5671 according to the formula:

$$K_i = \frac{IC_{50}}{1 + \frac{L}{K_d}}$$

A_2 K_i values were calculated from the IC_{50} values for unlabeled NECA (15.3 nM) and CPA (685 nM) by the equation

$$K_i = \frac{IC_{50}}{1 + \frac{L}{K_d} + \frac{C}{K_c}}$$

where C is the concentration of CPA (50 nM) and K_c is its affinity. In this case, two simultaneous equations in two variables had to be solved to derive the final multiplier, 0.6745.

Other models which were used in fitting of curves are the following. 1) the cooperative (logistic) model:

$$Y = T - S \cdot \frac{D^Q}{D^Q + K^Q}$$

where Y, T, S, D, and K are the same as in the Langmuir equation and Q is a cooperativity (pseudo-Hill) coefficient. 2) The two-site mass-action (Langmuir 2) model:

$$Y = T - S_1 \cdot \frac{D}{D + K_1} - S_2 \cdot \frac{D}{D + K_2}$$

3) The DISP1 model, a two-site model for dose-inhibition curves in the presence and absence of 50 nM CPA, assuming that CPA has 1.0 nM affinity at A_1 and 700 nM affinity at A_2 sites,[2] and assuming that the test agent has the same affinity at both sites:

$$Y = T - S_1 \cdot \frac{D}{D + K \cdot \left(1 + \frac{C}{1.0}\right)} - S_2 \cdot \frac{D}{D + K \cdot \left(1 + \frac{C}{700}\right)}$$

where Y, T, S, D, and K are as defined above, and C is the concentration of CPA (0 nM or 50 nM). 4) The DISP2 model, which is the same as DISP1 except that the test agent has different affinities at the two sites:

$$Y = T - S_1 \cdot \frac{D}{D + K_1 \cdot \left(1 + \frac{C}{1.0}\right)} - S_2 \cdot \frac{D}{D + K_2 \cdot \left(1 + \frac{C}{700}\right)}$$

5) The n-site saturation model with unlabeled ligand and a competing drug:

$$Y = B + N \cdot L + \sum_{j=1}^{n} M_j \cdot \frac{L}{L + K_j \cdot \left(1 + \frac{U}{K_j} + \frac{D}{I_j}\right)}$$

where Y is bound radioligand, B is the counting blank, N is the coefficient for nonspecific binding, L is the radioligand concentration, M_j is the B_{max} for the jth site, K_j is the K_d of the radioligand at the jth site, U is the concentration of unlabeled ligand, D is the concentration of the competing drug, and I_j is the K_i of the competing drug at the jth site. All units are expressed in nM, except for N, which is unitless. Free radioligand was assumed equal to total radioligand in this analysis; in the actual experiments, bound radioligand was always less than 5% of total radioligand.

Goodness of fit was expressed as the reduced χ^2 value, χ^2_v which is the weighted sum of squares divided by the number of degrees of freedom (a χ^2_v value significantly greater than 1.0 implies that the model does not completely describe the data). Different models were compared for statistical differences in goodness of fit by the F test for incremental improvement with addition of another term (23).

Results

[^{3}H]NECA binding assay. Our initial experiments studying inhibition of [^{3}H]NECA binding by adenosine analogs (Fig. 2, A–D) in rat striatal membranes confirmed that [^{3}H]NECA binds to two sites, both of which have nanomolar affinity for several adenosine agonists and therefore are likely to be adenosine receptors. CHA and *R*-PIA, which are known to be highly A_1-selective, gave the greatest separation in affinities at the two sites, whereas the less selective 2-chloroadenosine had a smaller but statistically significant separation (see Fig. 2 legend). Although the concentration-inhibition curve for unlabeled NECA fit a two-site model better than a one-site model, the second site appeared to be the low affinity "nonreceptor" site which has been described previously (20) (this site is characterized in more detail later in this paper). NECA thus appeared to have roughly equal affinities at the two adenosine receptor sites. The affinities of nucleosides for the higher affinity site were almost identical to their affinities at A_1

[2] Actual IC_{50} values for CPA were 1.07 nM and 685 nM.

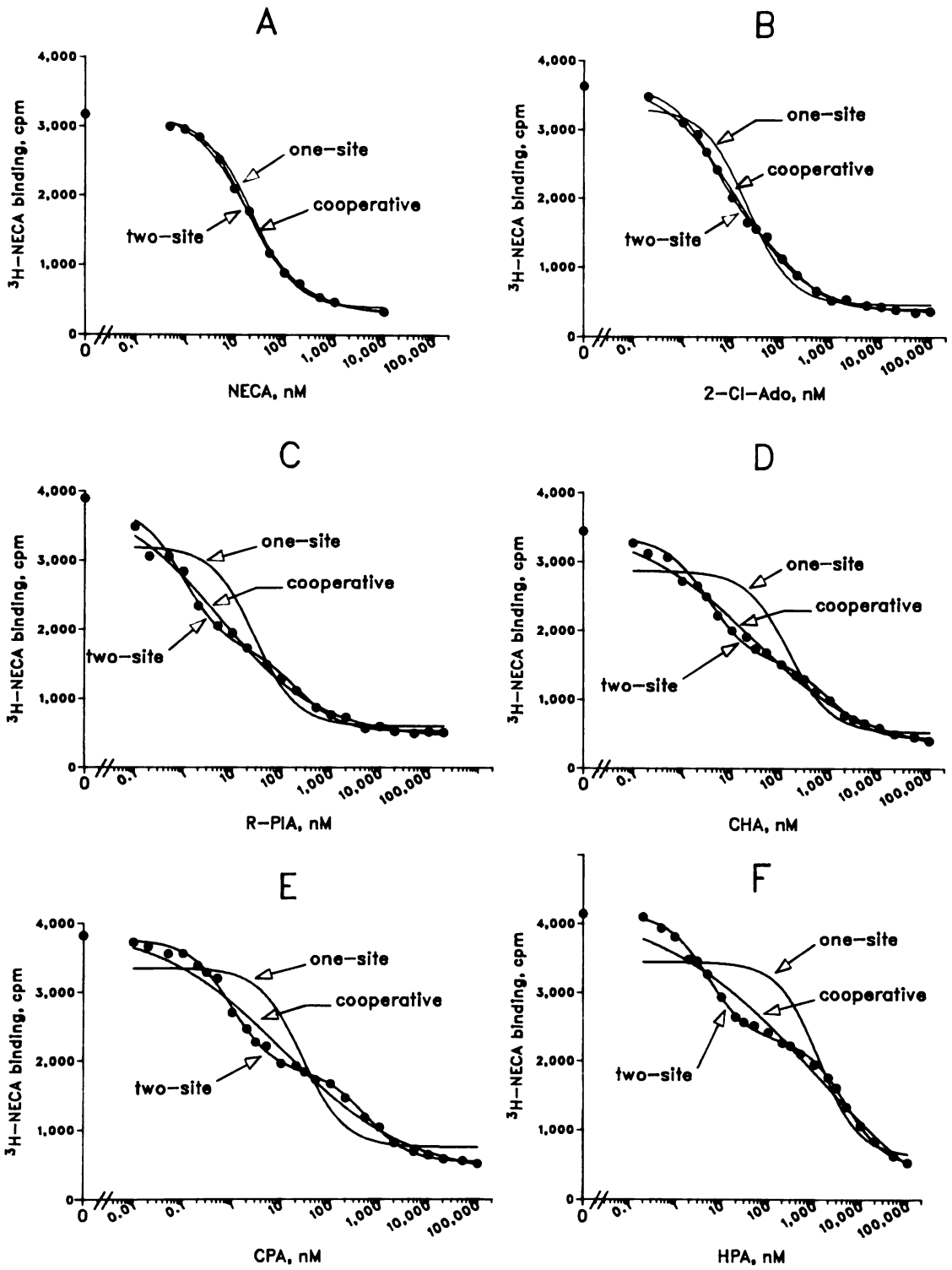

Fig. 2. "Best-fit" dose-inhibition curves for adenosine agonists versus [^{3}H]NECA in rat striatal membranes using the one-site (Langmuir), cooperative (logistic), and two-site (Langmuir 2) models. Models are described in Experimental Procedures. Data points for each compound are means of triplicate incubations from a single experiment. The CHA and CPA experiments were done three times with essentially identical results. Incubation conditions were as described in Experimental Procedures except that 50 nM CPA was omitted. χ^2_ν is the weighted sum of squares divided by the number of degrees of freedom. In all experiments, the cooperative and two-site models gave better fits ($p < 0.001$, F test) than the one-site model. A three-site Langmuir model did not give a significantly better fit than the two-site model for any compound.

receptors in [^{3}H]CHA binding (7), whereas their affinities at the site with the lower affinity for CHA and *R*-PIA were highly suggestive of an A_2 receptor.[3]

In order to observe the binding of [^{3}H]NECA to presumptive A_2 sites in the absence of the confounding influence of A_1 binding, it was necessary to devise a method to selectively eliminate the A_1 component of binding. Although CHA was the most A_1-selective of the common reference adenosine agonists, it did not provide a satisfactory solution to the problem, since the concentration-inhibition curve for CHA did not have a clear plateau region separating the A_1 and A_2 phases of inhibition. This is illustrated by the fact that the two-site (Langmuir 2) model did not give a statistically better fit than the cooperative (logistic) model (see Fig. 2 legend).

Yeung and Green (20) pretreated rat striatal membranes with *N*-ethylmaleimide to eliminate A_1 binding of [^{3}H]NECA. Using displacement with 100 nM CHA as a rough indicator of A_1 versus A_2 binding, we found that, although apparent A_1 binding was inhibited, apparent A_2 binding actually increased. This was later confirmed using 50 nM CPA to differentiate A_1 and A_2 binding (Fig. 3). These results suggest that *N*-ethylmaleimide may also have effects on A_2 receptors, possibly by a "locking" mechanism as previously described for β-adrenergic receptors (24). We also found *N*-ethylmaleimide to be about 30-fold more potent than in the study by Yeung and Green (20). These differences are likely to be due to the fact that we added the *N*-ethylmaleimide to the incubation itself, whereas Yeung and Green (20) added the *N*-ethylmaleimide to a more concentrated membrane suspension during a preincubation.

As CPA was about twice as potent as CHA in [^{3}H]CHA binding (25), this compound was examined for its ability to differentiate A_1 and A_2 components of binding (Fig. 2E). The CPA dose-inhibition curve had a clearly discernable plateau between the A_1 and A_2 phases of incubation, and, in contrast to the results with CHA, the two-site Langmuir model gave a markedly better fit than the cooperative model (see Fig. 2 legend). A concentration of 50 nM CPA was chosen to be added to all A_2 binding assays to eliminate A_1 binding. From the K_i values for CPA and NECA (see Table 1 later in this paper), it can be calculated that 50 nM CPA will occupy 98% of A_1 receptors while sparing 93% of A_2 receptors.

In addition to 50 nM CPA, the standard A_2 binding assay contained 10 mM $MgCl_2$; this concentration of $MgCl_2$ increased A_2 binding and also decreased nonspecific binding (illustrated in Table 4 later in this paper). Under the standard binding protocol, with 120,000 cpm of [^{3}H]NECA, specific A_2 binding is about 1,500 cpm and nonspecific binding is about 400 cpm. An additional 1,500 cpm of A_1 binding is observed if CPA is omitted. Nonspecific binding was the same whether defined by 100 μM CPA, 100 μM 2-chloroadenosine, or a combination of 100 nM CHA and 1 mM theophylline (data not shown). A high (10 μM) concentration of NECA was able to decrease binding by an additional 120 cpm, in agreement with the results of Yeung and Green (20). Specific A_2 binding was linear with tissue up to 20 mg of original wet weight (data not shown).

Requirement for adenosine deaminase. A_1 receptor binding assays require the presence of adenosine deaminase to eliminate endogenous adenosine, which is continually generated by the membranes (7–9). To determine the requirement for adenosine deaminase in the A_2 binding assay, we examined the effects of pentostatin (2′-deoxycoformycin), an adenosine deaminase inhibitor with an affinity constant of 2.5 pM (26). Pentostatin was a partial inhibitor of binding, reducing specific

[3] For convenience, the component of specific binding remaining after A_1 binding is eliminated is referred to here as A_2, although the evidence supporting this designation is not presented until later in this paper.

Fig. 2 Legend—cont'd.

Model	Binding (cpm)			IC_{50} (nM)		Cooperativity	χ^2_v
	Specific		Nonspecific	Site 1	Site 2		
	Site 1	Site 2					
			A. NECA				
One-site	2684		386	22.9			2.34
Cooperative	2895		325	18.4		0.786	1.243
Two-site	2570	265	306	16.3	796		0.973
			B. 2-Chloroadenosine				
One-site	2848		460	20.1			4.83
Cooperative	3335		353	11.8		0.598	1.078
Two-site	2129	1095	391	3.95	151		0.993
			C. R-PIA				
One-site	2601		594	28.3			12.6
Cooperative	3474		431	5.44		0.416	1.483
Two-site	2043	1193	523	0.999	210		1.808
			D. CHA				
One-site	2349		520	144			12.3
Cooperative	3278		242	26.6		0.362	1.258
Two-site	1797	1132	425	3.28	1030		1.553
			E. CPA				
One-site	2610		739	26.7			37.1
Cooperative	3612		340	10.7		0.340	4.62
Two-site	1930	1301	529	0.956	542		1.313
			F. N^6-(3-Hydroxypropyl)adenosine				
One-site	2948		454	1890			18.8
Cooperative	3655		354	305		0.401	5.86
Two-site	1849	1869	404	5.63	5590		1.315

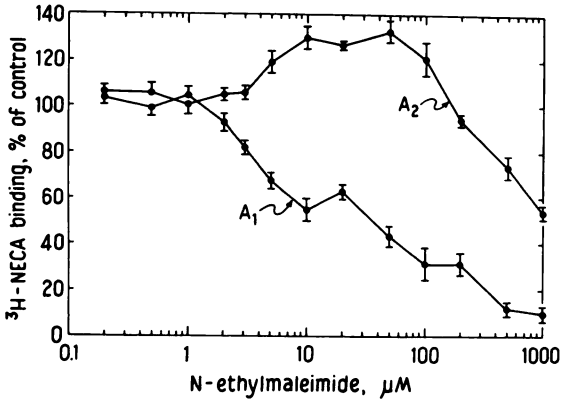

Fig. 3. Effects of *N*-ethylmaleimide on A_1 and A_2 binding of [^{3}H]NECA. Binding was performed as described in Experimental Procedures. *N*-Ethylmaleimide, [^{3}H]NECA, and CPA were added first to the tube, and the incubation was initiated by addition of the membrane suspension. A_1 binding was defined as total binding minus binding in the presence of 50 nM CPA, and A_2 binding was defined as binding in the presence of 50 nM CPA minus binding in the presence of 100 μM CPA. Values are means ± SE of triplicate incubations from a representative experiment. A_2 binding in the presence of 5, 10, 20, 50, or 100 μM *N*-ethylmaleimide was significantly higher than in the absence of *N*-ethylmaleimide (5, 10, 20, 50 μM, $p < 0.01$; 100 μM, $p < 0.05$; one-sided *t* test).

A_2 binding by 70%, compared to an 89% maximal inhibition of specific [^{3}H]CHA binding to A_1 receptors (Fig. 4). The concentration-inhibition curves were extremely steep, with cooperativity coefficients of 6 in A_2 binding and 9 in A_1 binding. This "threshold" phenomenon is undoubtedly due to the stoichiometric interaction between pentostatin and adenosine deaminase: since the amount of adenosine deaminase used in this study (0.1 unit/ml) is at least 10-fold in excess of the concentration needed to give maximal enhancement of binding,[4] inhibition of up to 90% of the adenosine deaminase would have no effect on binding, but a very small additional increase in pentostatin would result in total inhibition of the deaminase and a maximal inhibition of binding. In agreement with this titration model, changing the adenosine deaminase concentration results in corresponding changes in the threshold for inhibition of binding by pentostatin (data not shown).

Time course. Binding of [^{3}H]NECA to A_2 receptors was half complete at about 20 min (Fig. 5). Least squares analysis of the association was complicated by the fact that the nonspecific binding also demonstrated association kinetics. It was necessary to add an extra exponential statement for time-dependent nonspecific binding in addition to the one (ASOC1A) or two (ASOC2A) exponential phases of specific binding. Without parameters for time-dependent nonspecific binding, reduced χ^2 values were exorbitantly high (>15); even with the additional parameters, χ^2_ν for the ASOC2A model was several times the expected value of 1.0, indicating a suboptimal fit (see Fig. 5 legend). The time-dependent nonspecific binding probably represents the low affinity "nonreceptor" component of [^{3}H]NECA binding. The biexponential model (ASOC2A) gave a significantly better fit ($p < 0.01$) than the monoexponential (ASOC1A) model. Best fit parameters were $t_{1/2}$ 2.3 min, 40% of specific binding, and $t_{1/2}$ 32 min, 60% of specific binding. Dissociation experiments also fit two (or more) sites, with $t_{1/2}$ of 5.0 min (40%) and 137 min (60%) (Fig. 5). Nonspecific binding showed negligible dissociation, presumably because the low affinity binding site remained at equilibrium under the conditions of the dissociation protocol.

[4] R. F. Bruns, G. H. Lu, and T. A. Pugsley, unpublished results.

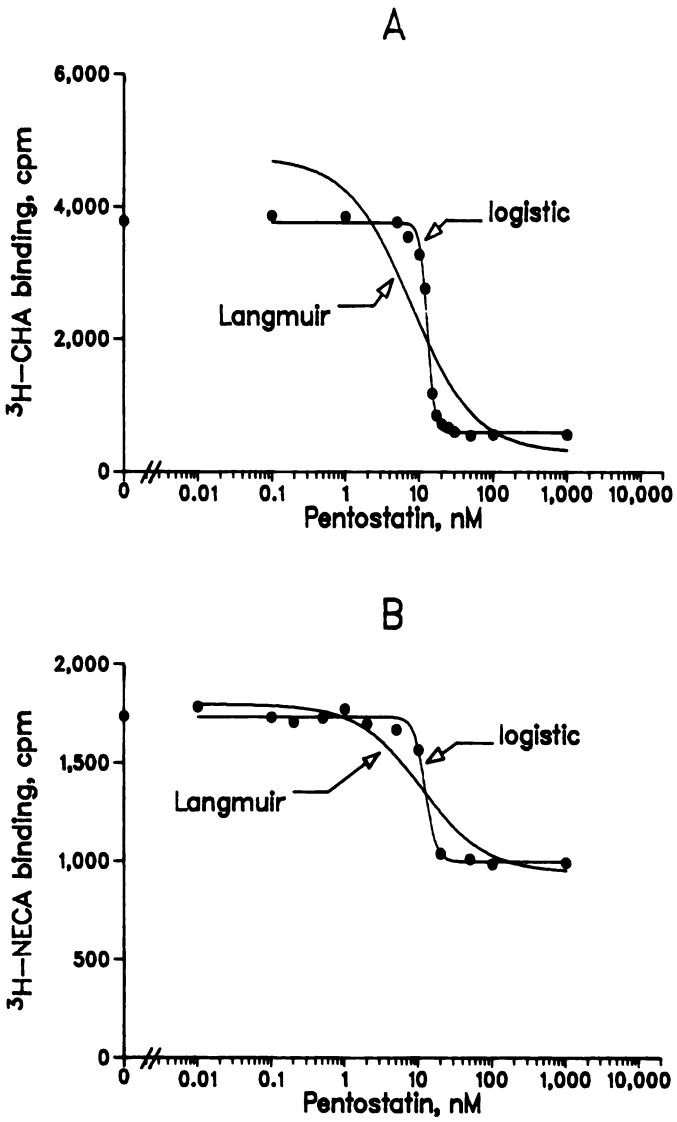

Fig. 4. Concentration-inhibition curves for pentostatin (2′-deoxycoformycin) versus [^{3}H]CHA and [^{3}H]NECA binding. Binding of [^{3}H]CHA to A_1 receptors and of [^{3}H]NECA to A_2 receptors was performed as described in Experimental Procedures. The membrane suspensions contained sufficient adenosine deaminase for a final concentration of 0.1 unit/ml (manufacturer's specifications), and were added last to the tubes. Results are total binding and are typical of experiments repeated at least three times. "Best fit" parameter values are given below. χ^2_ν is the weighted sum of squares divided by the number of degrees of freedom. Nonspecific binding was 194 cpm for [^{3}H]CHA and 305 cpm for [^{3}H]NECA.

Model	Ligand	Binding		K_d (nM)	Cooperativity	χ^2_ν
		Noninhibitable (cpm)	Inhibitable (cpm)			
Langmuir	[^{3}H]CHA	291	4450	7.79		122.6
Logistic	[^{3}H]CHA	594	3160	12.85	8.68	2.449
Langmuir	[^{3}H]NECA	852	944	11.01		6.19
Logistic	[^{3}H]NECA	736	997	12.34	5.69	1.034

Saturation. Receptors which are linked to adenylate cyclase generally exist in two or more coupling states, which differ in

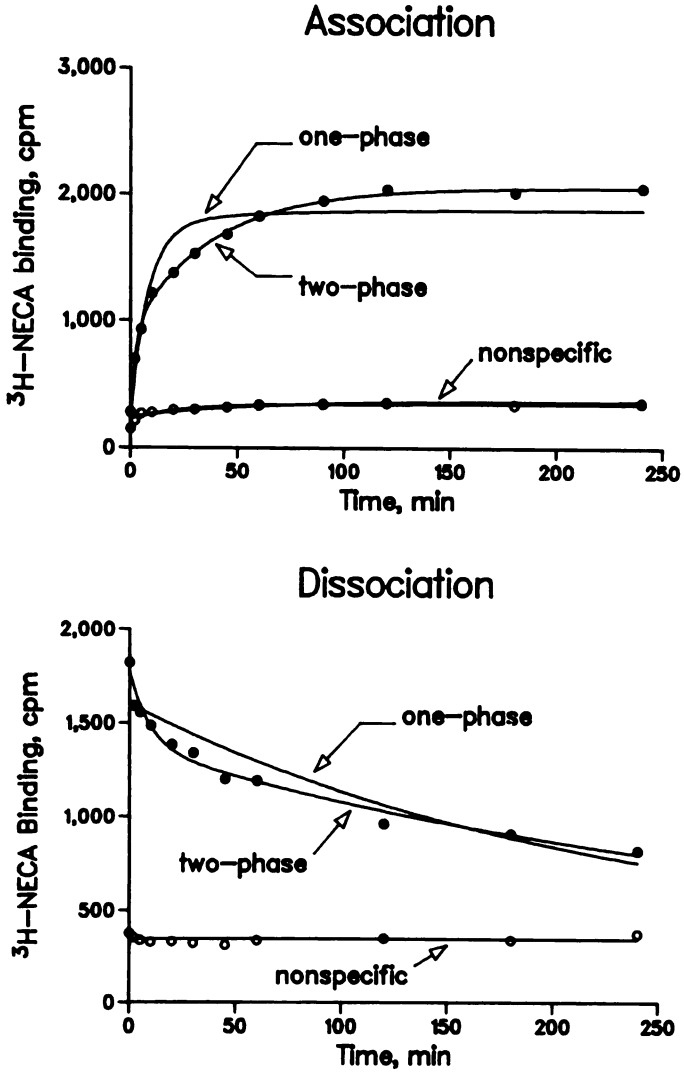

Fig. 5. Association and dissociation kinetics for [^{3}H]NECA binding to A_2 receptors. Incubations (duplicate) were performed as described in Experimental Procedures. For association, ligand and CPA (50 nM or 100 μM final concentration) were added to tubes in a volume of 110 μl, and incubations were initiated by addition of 890 μl of membranes at appropriate times, followed by simultaneous filtration of all the samples on a Brandel 48R cell harvester. Results from a typical experiment are given in the figure; the *curves* are "best fit" results for the ASOC1A and ASOC2A models. Mean best fit values ± interexperimental standard error for three independent experiments are given below. χ^2_ν (the weighted sum of squares divided by the number of degrees of freedom) is the aggregate value for the three experiments. For the dissociation kinetics, ligand and CPA (50 nM or 100 μM final concentration) were added to tubes in a volume of 100 μl, and incubations were initiated by addition of 890 μl of membranes at appropriate times; after a tube had incubated for 60 min, dissociation was initiated by addition of 10 μl of 10 mM CPA (added to both specific and nonspecific tubes) and the tube was incubated for a further period, after which all tubes were simultaneously filtered on a Brandel 48R cell harvester. Results from a typical experiment are given in the figure; the *curves* are the "best fit" results for the DSOC1 and DSOC2 models. Mean parameter values ± interexperimental SE for four independent experiments are given below. χ^2_ν is the aggregate value for the four experiments.

Model	Constant nonspecific (cpm)	Time-dependent nonspecific		Specific				χ^2_ν
				Site 1		Site 2		
		cpm	$t_{1/2}$ (min)	cpm	$t_{1/2}$ (min)	cpm	$t_{1/2}$ (min)	
ASOC1A	164 ± 102	245 ± 117	43 ± 22	1780 ± 256	8.0 ± 2.3			8.97
ASOC2A	196 ± 53	199 ± 85	16 ± 4	800 ± 74	2.3 ± 0.5	1200 ± 192	32 ± 2	4.10
DSOC1	338 ± 14			1408 ± 72	79 ± 24			8.07
DSOC2	329 ± 11			685 ± 152	5.0 ± 0.6	1011 ± 115	137 ± 32	1.92

their affinities for agonists (see Refs. 22 and 27 and references therein). Affinities of antagonists at the different coupling states either are unchanged or vary inversely with agonist affinities. It could therefore be predicted that as many as five different [^{3}H]NECA-binding sites would exist in rat striatum: two coupling states of the A_1 receptor, two coupling states of the A_2 receptor, and the low affinity, high capacity "nonreceptor" site. In light of this prediction, it is not surprising that attempts to fit saturation data for [^{3}H]NECA to a simple two-site model gave ambiguous results: each of three experiments

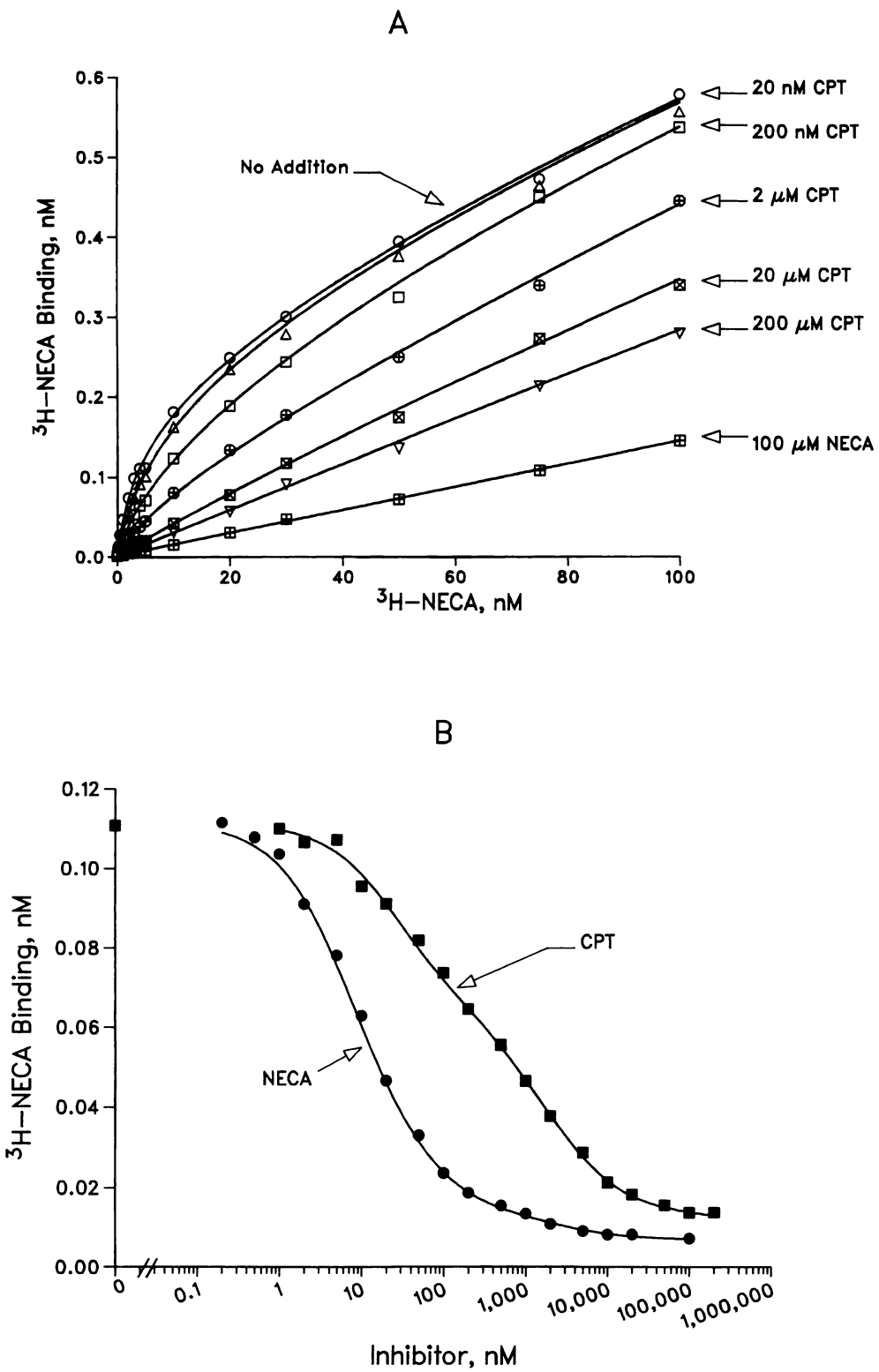

Fig. 6

gave two distinct minima on the least squares surface. In order to fully identify the different [^{3}H]NECA binding sites, a large (480 incubations) saturation/competition experiment was performed (Fig. 6). Saturation curves for 0.2–100 nM [^{3}H]NECA were performed alone, with 100 μM NECA, and with six different concentrations of CPT, an A_1-selective antagonist (see Table 1 later in this paper). CPT was chosen because, as an antagonist, its affinity should remain about the same at a given receptor regardless of the coupling state. Concentration-inhibition curves for CPT (1 nM–200 μM) and unlabeled NECA (0.2 nM–100 μM) versus 4 nM [^{3}H]NECA were also carried out as part of the same experiment. The concentration-inhibition curve for unlabeled NECA was included in order to obtain information about the saturation of the low affinity "nonreceptor" NECA-binding site. In each of two experiments, a four-site model gave the best fit ($p < 0.001$ compared to three-site model, F test). It was possible to identify the four sites unambiguously by their affinities for CPT, a high (10 nM) affinity indicating an A_1 receptor, a moderate (1 μM) affinity indicating an A_2 receptor, and a low (1 mM) affinity indicating a "nonreceptor" site. The four sites were identified as a high affinity A_1 receptor (NECA K_d 1.8 nM, CPT K_i 7.8 nM), a high affinity A_2 receptor (NECA 3.5 nM, CPT 1.2 μM), a low affinity A_2 receptor (NECA 35 nM, CPT 0.4 μM), and a high capacity "nonreceptor" site (B_{max} 1000 pmol/g of wet weight, NECA 3 μM, CPT 900 μM). Presumably, the predicted low affinity A_1 site was not observed because its numerical contribution to total binding was too small to be detected.

From the "best fit" parameter values in the legend to Fig. 6, it can be calculated that about 67% of the specific binding of 4 nM [^{3}H]NECA in the presence of 50 nM CPA will be to the high affinity A_2 receptor, with the remaining 33% belonging to the low affinity A_2 receptor. This 67:33 ratio is in reasonably good agreement with the 60:40 ratio of slowly to rapidly equilibrating sites observed in the association and dissociation experiments in Fig. 5.

Fig. 6. Saturation of [^{3}H]NECA binding in the presence of different concentrations of CPT. A. [^{3}H]NECA saturation curves (0.2–100 nM) carried out alone, in the presence of 100 μM NECA, and in the presence of 20 nM, 200 nM, 2 μM, 20 μM, or 200 μM concentrations of CPT. (An additional curve for 2 nM CPT was included in the curve-fitting analysis but omitted from the figure.) B. Dose-inhibition curves for unlabeled NECA (0.2 nM–100 μM) and CPT (1 nM–200 μM) against 4 nM [^{3}H]NECA (performed as part of the same experiment and included in the nonlinear least squares analysis). Incubation conditions were as described in Experimental Procedures except that the 50 nM CPA was omitted. The data are from a typical experiment which was repeated with essentially identical results; the curves are the "best fit" solution to the four-site saturation/competition model. Aggregate χ_ν^2 values (weighted sum of squares divided by degrees of freedom) of the different models for the two experiments were: one site, 14.0; two-site, 4.74; three-site, 1.50; four-site, 0.915. The four-site model gave a significantly better fit than the three-site model in both experiments ($p < 0.001$, F test). The five-site model failed to converge in one experiment and failed to give an improved χ^2 value in the other experiment ($p > 0.05$, F test). Mean best fit parameter values for the four-site model from the two experiments are given below along with the interexperiment standard error values. B_{max} is expressed as pmol/g of wet weight.

	Counting blank (1.40 ± 0.02 pM)	Nonspecific binding (0.146 ± 0.006 %)	
	B_{max} (pmol/g)	NECA K_d (nM)	CPT K_i (nM)
Site 1	11.8 ± 2.8	1.81 ± 0.59	7.85 ± 2.08
Site 2	14.2 ± 2.1	3.54 ± 0.44	1,180 ± 35
Site 3	36.0 ± 5.9	34.8 ± 6.2	386 ± 264
Site 4	995 ± 193	3,200 ± 690	921,000 ± 278,000

Structure-activity relationships at A_1 and A_2 receptors in rat brain. Affinities of compounds for putative A_2 receptors were compared with their affinities for A_1 receptors (Table 1). A_2 receptors were labeled by [^{3}H]NECA in the presence of 50 nM CPA in rat striatal membranes, and A_1 receptors were labeled by [^{3}H]CHA in rat whole brain membranes. The two receptors showed quite distinct structure-activity profiles. Although all of the N^6-modified adenosines had higher affinity for A_1 than for A_2 receptors, they varied markedly in the degree of their preference for A_1 receptors. N^6-(3-hydroxypropyl) adenosine had high A_1 selectivity, with an affinity ratio of 700, about the same as CPA. CHA was also highly A_1-selective. *R*-PIA was significantly less A_1-selective than CHA, due to its better affinity at A_2 receptors. *R*-PIA was 42-fold more potent than its diastereomer *S*-PIA at A_1 receptors, and 15-fold more potent at A_2 receptors. In contrast to the highly A_1-selective N^6-derivatives mentioned above, N^6-benzyladenosine had almost equal affinity in A_1 and A_2 receptor binding.

In the same way that certain N^6-substituents imparted a high degree of selectivity for A_1 receptors, bulky 2-position substituents were capable of endowing a modest degree of A_2 selectivity to adenosine (Table 1). CV-1808 was the most A_2-selective compound in the present study, exhibiting a 5-fold higher affinity for A_2 than for A_1 receptors. Compared to 2-chloroadenosine, CV-1808 was about 30-fold more selective for A_2 receptors. 2-Chloroadenosine is likely to have about the same affinity at A_1 and A_2 receptors as adenosine itself. Adenosine was not tested due to its susceptibility to adenosine deaminase.

NECA was the most potent compound at A_2 receptors, with a K_i of 10.3 nM; despite its high affinity for A_2 receptors, NECA had a 1.7-fold greater affinity for A_1 receptors than for A_2. The other potent members of the NECA family had about the same selectivity ratios as NECA, except for the methyl homolog of NECA, which was about twice as A_2-selective as the other members of the series. Several other 5′-derivatives of adenosine (e.g., 5′-methylthioadenosine) that were previously shown to have affinities of 5–20 μM as antagonists or partial agonists at the low affinity A_2 receptor in human fibroblasts (28) had slightly higher affinities at the high affinity A_2 receptor labeled by [^{3}H]NECA and had still higher affinities at A_1 receptors.

Numerous xanthines have been shown to block both A_1 and A_2 adenosine receptors. Most of the xanthines tested in the present study were severalfold more potent at A_1 than at A_2 receptors (Table 1). 8-(2-Amino-4-chlorophenyl)-1,3-dipropylxanthine and PD 113,297 had the highest affinity of the xanthines at the A_2 receptor but were, nevertheless, rather selective for A_1 receptors due to their very high affinity in [^{3}H]CHA binding (29, 30). 8-Cyclo-pentyltheophylline was the most A_1-selective antagonist, exhibiting 130-fold higher affinity at A_1 than at A_2 sites.

The only antagonist to show any degree of selectivity for A_2 receptors was the benzo[*g*]pteridine alloxazine (18), which exhibited 2 times higher affinity for A_2 receptors than for A_1. The non-xanthine adenosine antagonists tracazolate and cartazolate (11, 31) showed moderate affinity for both A_1 and A_2 sites.

N^6-(3-Hydroxypropyl)adenosine competition for [^{3}H]NECA binding in the presence and absence of CPA. The

TABLE 1

Affinities of adenosine agonists and antagonists for inhibition of A_1 and A_2 adenosine receptor binding in rat brain membranes

A_1 receptor binding was assayed using 1 nM [^{3}H]CHA in 2 ml of 50 mM Tris·HCl, pH 7.7, for 60 min at 25° with 20 mg original tissue wet weight of membranes from whole rat brain minus brainstem and cerebellum. A_2 receptor binding was assayed using 4 nM [^{3}H]NECA with 50 nM CPA in 1 ml of Tris with 10 mM $MgCl_2$ for 60 min at 25° with 5 mg original tissue wet weight of rat striatal membranes. Further details are provided in Experimental Procedures. IC_{50} values were computed using the Langmuir model (see Experimental Procedures). K_i values were calculated from IC_{50} values as described in Experimental Procedures. Values are means ± SE of *n* separate experiments.

Compound	A_1 K_i	*n*	A_2 K_i	*n*	K_i ratio (A_2/A_1)	Source[a]
	nM		nM			
N^6-Modified Nucleosides						
N^6-benzylado[b]	120 ± 21	5	285 ± 20	3	2.37	A
N^6-Methylado	364 ± 18	3	4,550 ± 420	3	12.5	A
N^6-[(*S*)-1-Methyl-2-phenylethyl]ado (*S*-PIA)	49.3 ± 2.4	4	1,820 ± 380	4	36.8	C2, E
N^6-[(*R*)-1-Methyl-2-phenylethyl]ado (*R*-PIA)	1.17 ± 0.16	5	124 ± 9	3	106	C3, E, F
N^6-(2-Hydroxyethyl)ado	18.1 ± 0.9	3	2,410 ± 590	3	133	G
N^6-Phenylado	4.62 ± 0.20	3	663 ± 82	3	144	B
N^6-[3-(4-Chlorophenyl)bicyclo[2.2.2]oct-2-yl]ado (EMD 28422)	19.3	1	6,330 ± 1,020	2	328	H
N^6-Cyclohexylado (CHA)	1.31 ± 0.12	4	514 ± 68	4	392	C3, E, I
N^6-(3-Hydroxypropyl)ado	7.01 ± 0.17	3	4,920 ± 340	4	702	C1
N^6-Cyclopentylado (CPA)	0.589 ± 0.019	4	462 ± 15	4	784	C1
2-Modified Nucleosides						
2-(Phenylamino)ado (CV-1808)	561 ± 40	3	119 ± 16	3	0.213	J
2-(4-Methoxyphenyl)ado (CV-1674)	1,320 ± 50	3	605 ± 23	3	0.458	J
2-Oxoado (isoguanosine)	94.1 ± 23.3	3	331 ± 44	3	3.52	G
2-Chloroado	9.33 ± 0.58	4	63.2 ± 7.5	3	6.77	A
5′-Modified Nucleosides						
Ado-5′-methylcarboxamide	83.6 ± 1.6	3	66.8 ± 15.6	3	0.800	K
Ado-5′-ethylcarboxamide (NECA)	6.26 ± 0.52	3	10.3 ± 0.5	4	1.64	C4, E
Ado-5′-carboxamide	72.6 ± 1.1	3	120 ± 15	3	1.66	G
Ado-5′-(2-hydroxyethyl)carboxamide	28.1 ± 0.6	3	57.5 ± 2.5	3	2.04	K
Ado-5′-cyclopropylcarboxamide	6.44 ± 0.56	3	13.4 ± 2.9	3	2.08	L
Ado-5′-ethylcarboxylate	174 ± 19	3	387 ± 16	3	2.22	C5
5′-Methylthioado	281 ± 15	3	1,100 ± 80	3	3.93	A
5′-*O*-Nitroado	60.9 ± 6.3	3	335 ± 43	3	5.51	M
Ado-5′-cyclohexylcarboxamide	635 ± 7	3	4,300 ± 520	3	6.77	K
5′-Deoxy-5′-iodoado	92.8 ± 8.1	3	637 ± 110	3	6.86	N
5′-*O*-Acetylado	584	1	4,510 ± 240	2	7.72	O
2- and 5′-Modified Nucleosides						
2-Chloro-5′-methylthioado	206 ± 9	3	1,880 ± 240	4	9.12	P
Miscellaneous Nucleosides						
2′-Deoxy-N^6-methylado	26,000 ± 170	2	>100,000	1		A
9-Deazaado	>10,000	2	>100,000	1		Q
6-[(2-Hydroxy-5-nitrobenzyl)thio]inosine	43,200 ± 1,100	3	34,700 ± 5,600	3	0.803	I
7-Thia-9-deazaado	18,500	1	34,100	1	1.84	Q
1-Methyl-2-oxoado	150 ± 8	3	3,250 ± 90	3	21.7	C1
$1,N^6$-Etheno-2-oxoado	760	1	48,200	1	63.5	R
Xanthines						
1-(5-Oxohexyl)theobromine (pentoxifylline)	>100,000	1	>100,000	1		AA
Caffeine (1,3,7-trimethylxanthine)	29,100 ± 1,200	3	48,100 ± 2,800	3	1.65	A
1-Ethyltheobromine	20,700 ± 1,000	3	37,700 ± 2,500	3	1.82	S
7-(2-Chloroethyl)theophylline	8,170 ± 708	3	15,000 ± 2,000	3	1.84	N
Theobromine (3,7-dimethylxanthine)	83,400 ± 11,000	4	187,000 ± 18,000	3	2.24	A
1-Butyltheobromine	13,000 ± 3,000	3	35,900 ± 700	3	2.75	S
Theophylline (1,3-dimethylxanthine)	8,470 ± 1,490	3	25,300 ± 2,000	3	2.99	A
1-Methylxanthine	11,400 ± 1,600	3	36,200 ± 800	3	3.18	T
3-Propylxanthine (enprofylline)	29,100 ± 2,500	3	103,000 ± 17,000	3	3.56	U
3-Isobutyl-1-methylxanthine	2,460 ± 210	3	13,800 ± 900	3	5.60	N
8-(4-Sulfophenyl)theophylline	2,630 ± 100	3	15,300 ± 900	3	5.80	C4, D, E
8-(4-Aminophenyl)theophylline	65.2 ± 4.2	3	391 ± 10	3	5.99	D
8-(4-Chlorophenyl)theophylline	47.7 ± 2.1	3	371 ± 28	3	7.79	V
8-(2-Furyl)theophylline	350 ± 20	4	2,780 ± 50	3	7.94	D
1,3-Diethylxanthine	2,710 ± 160	3	22,200 ± 3,800	3	8.19	W
8-(4-Methoxyphenyl)theophylline	44.4 ± 2.4	3	419 ± 18	3	9.42	V
8-Phenyltheophylline	86.0 ± 2.8	3	848 ± 115	3	9.85	E, I, V
1,3-Dipropylxanthine	450 ± 25	3	5,160 ± 590	3	11.5	W
8-(4-Carboxyphenyl)theophylline	610 ± 125	3	7,260 ± 810	3	11.9	D
8-(2,4-Diaminophenyl)-1,3-dipropylxanthine	17.6 ± 1.4	3	214 ± 28	3	12.2	D
8-[4-[*N*-(3-Dimethylaminopropyl)-sulfonamido]phenyl]-1,3-Dipropylxanthine (PD 113,297)	5.59 ± 0.39	3	70.0 ± 2.8	3	12.5	C4

TABLE 1—*Continued*

Compound	A_1 K_i	n	A_2 K_i	n	K_i ratio (A_2/A_1)	Source[a]
	nM		nM			
8-(3-Furyl)theophylline	72.4 ± 3.7	3	984 ± 70	3	13.6	D
8-(2-Thienyl)theophylline	96.8 ± 3.2	3	1,580 ± 30	3	16.4	D
8-(2-Aminophenyl)theophylline	82.9 ± 15.0	4	1,430 ± 40	3	17.2	D
1,3-Dipropyl-8-phenylxanthine	10.2 ± 2.6	4	180 ± 29	3	17.8	D
1,3-Diethyl-8-phenylxanthine (DPX)	44.5 ± 1.2	3	863 ± 73	3	19.4	D, E
8-(4-Nitrophenyl)theophylline	112 ± 6	3	2,520 ± 150	3	22.5	V
8-Propyltheophylline	367 ± 10	3	10,000 ± 300	3	27.3	X
8-(2-Amino-4-chlorophenyl)-1,3-dipropylxanthine	2.51 ± 0.06	4	91.9 ± 6.8	4	36.7	C4, D, E
8-Cyclopentyltheophylline (CPT)	10.9 ± 0.9	4	1,440 ± 70	3	133	C4, X
Miscellaneous Non-nucleosides						
Alloxazine	5,250 ± 440	3	2,720 ± 160	3	0.517	N
Tracazolate	542 ± 9	3	1,560 ± 180	3	2.88	Y
Cartazolate	357 ± 40	3	2,240 ± 310	3	6.28	Z

[a] Key to sources of compounds: **A**, Sigma Chemical Co. **B**, Dr. M. H. Fleysher (deceased), Roswell Park Memorial Institute, Buffalo, NY 14203. **C**, Cardiotonics/Adenosine Section, Dr. James Bristol, Director, Department of Chemistry, Warner-Lambert/Parke-Davis, Ann Arbor, MI 48105; **C1**, Dr. Walter Moos; **C2**, Dr. Harriet Hamilton; **C3**, Dr. James Bristol; **C4**, Mr. Edward Badger; **C5**, Mr. William Patt. **D**, synthesized by R. F. B. (Ref. 29). **E**, Research Biochemicals, Inc., Post Office Box 181, Wayland, MA 01778. **F**, Boehringer-Mannheim. **G**, Drug Research and Development, NCI, NIH, Bethesda, MD 20205. **H**, E. Merck Darmstadt, Darmstadt, FRG. **I**, Calbiochem-Behring. **J**, Takeda Chemical Industries, Central Research Division, Osaka, Japan. **K**, Dr. Karl Dietmann (deceased), Medizinischer Forschung, Boehringer Mannheim GmbH, 68 Mannheim 21, FRG. **L**, Dr. John W. Daly, Laboratory of Bioorganic Chemistry, NIADDK, NIH, Bethesda, MD 20205. **M**, Dr. R. Duschinsky, Swiss Institute for Experimental Cancer Research, 1011 Lausanne, Switzerland. **N**, Aldrich Chemical Co. **O**, Dr. Hartmutt Follmann, Fachbereiche Chemie, Philipps-Universitat Marburg, D-3550 Marburg-Lahn, FRG. **P**, Dr. John Montgomery, Southern Research Institute, Birmingham, AL 35205. **Q**, Dr. Robert S. Klein, Laboratory of Organic Chemistry, Sloan-Kettering Institute for Cancer Research, New York, NY 10021. **R**, Dr. Kwan-Chung Tsou, 1515 Ravdin Institute, Hospital of the University of Pennsylvania, Philadelphia, PA 19174. **S**, Dr. E. Schraven, Department of Biological and Medical Research, Casella Farbwerke Mainkur AG, 6-Frankfurt-Fechenheim, Hanauer Lanstr. 526, FRG. **T**, Tridom-Fluka. **U**, Dr. Carl Persson, AB Draco, Research and Development Department, Box 34, S-221 00 Lund, Sweden. **V**, Dr. Edward C. Taylor, Department of Chemistry, Princeton University, Princeton, NJ 08540. **W**, Dr. Kurt J. Rorig, Associate Director, Chemical Research, Searle Laboratories, Box 5110, Chicago, IL 60680. **X**, Dr. Herman H. Stein, Abbott Laboratories, North Chicago, IL 60064. **Y**, Stuart Pharmaceuticals, Wilmington, DE 19897. **Z**, Squibb Institute for Medical Research, Princeton, NJ 08540. **AA**, Dr. V. Stefanovich, Hoechst Aktiengesellschaft, Werk Albert, Pharmazeutische Abteilung, Postfach 129101, 6200 Wiesbaden 12, West Germany.

[b] ado, adenosine.

results in Table 1 predict that N^6-(3-hydroxypropyl)adenosine should show as good a separation as CPA in the two-site model of [^{3}H]NECA binding. As shown in Fig. 2F, N^6-(3-hydroxypropyl)adenosine has a slightly better separation than CPA between the A_1 and A_2 components of the concentration-inhibition curve. When concentration-inhibition curves for N^6-(3-hydroxypropyl)adenosine generated in the presence and absence of 50 nM CPA are fit simultaneously to the DISP2 model (see Experimental Procedures), it is apparent that 50 nM CPA completely eliminates the high affinity (A_1) component of the N^6-(3-hydroxypropyl)adenosine concentration-inhibition curve (Fig. 7).

Regional distribution of the A_1 and A_2 components of [^{3}H]NECA binding. Significant A_1 and A_2 binding of [^{3}H]NECA was detected in all brain areas examined (Table 2). In agreement with binding and adenylate cyclase studies (11, 32), A_1 binding was rather broadly distributed. In contrast, A_2 binding was high only in the striatum and was quite low in all other brain regions. The apparent A_2-binding sites (defined as specific binding in the presence of 50 nM CPA) in nonstriatal tissue were not sufficiently abundant for further characterization.

Organ distribution of [^{3}H]NECA binding. Binding of [^{3}H]NECA was examined in several rat organs (Table 3). Excluding the brain, the only organ to exhibit a high degree of adenosine receptor binding was the testis. As expected (9, 11), the binding was to A_1 receptors, since it was eliminated by 50 nM CPA. A small amount (121 cpm) of apparent A_2 binding, defined as cpm for 50 nM CPA minus cpm for 100 μM CPA, was detected in the spleen. Several tissues, most notably liver, exhibited binding which could be displaced by 100 μM NECA but not 100 μM CPA; this presumably represents binding to the low affinity NECA-binding site, which is probably not an adenosine receptor (see below). Theophylline inhibited part of the low affinity NECA binding in several tissues (Table 3).

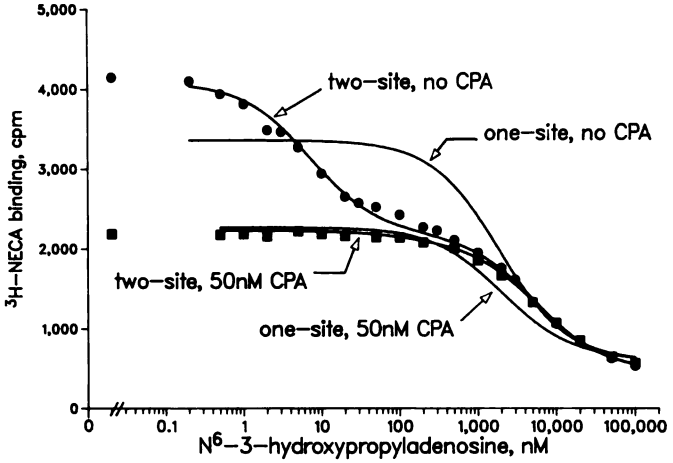

Fig. 7. N^6-(3-Hydroxypropyl)adenosine inhibition of [^{3}H]NECA binding to rat striatal membranes in the presence and absence of 50 nM CPA. *Points* are means of triplicate incubations, performed as described in Experimental Procedures. The *curves* are the "best fit" solutions for the DISP1 and DISP2 models.

Model	Binding (cpm)			IC_{50} (nM)		χ^2_ν
	Specific		Nonspecific	Site 1	Site 2	
	Site 1	Site 2				
DISP1	1055	1800	470	2620		13.5
DISP2	1909	1761	414	7.33	6300	1.175

Pharmacological specificity of the low affinity [^{3}H]NECA binding site. Unlabeled NECA was able to lower [^{3}H]NECA binding below the level of nonspecific binding, defined as binding in the presence of 100 μM CPA (Table 4). As

TABLE 2

Regional distribution of the A_1 and A_2 components of [^{3}H]NECA binding in rat brain

Brain regions were dissected from 200-g male Long-Evans rats and membranes were prepared according to Experimental Procedures and frozen. "Forebrain" is the same preparation used for [^{3}H]CHA binding (whole brain minus cerebellum and brainstem); "frozen striatum" refers to striatum prepared from frozen brains from Pel-Freez. All incubations (triplicate) were as described in Experimental Procedures: 5 mg of tissue, 4 nM [^{3}H]NECA (121,000 cpm). A_1 binding was defined as total binding minus binding in the presence of 50 nM CPA. A_2 binding was defined as binding in the presence of 50 nM CPA minus nonspecific binding in the presence of 100 μM CPA. The standard error of the difference of two means is calculated as the square root of the sum of the squares of the two standard errors. This experiment was performed two additional times with essentially identical results.

Region	[^{3}H]NECA binding (cpm ± SE)		
	Specific		Nonspecific
	A_1	A_2	
Striatum	1337 ± 61	1247 ± 29	353 ± 10
Cortex	1017 ± 31	144 ± 13	303 ± 12
Hippocampus	2004 ± 50	124 ± 16	340 ± 9
Thalamus	1456 ± 31	144 ± 23	373 ± 4
Hypothalamus	637 ± 24	103 ± 25	312 ± 18
Brainstem	477 ± 25	71 ± 24	288 ± 15
Cerebellum	772 ± 27	87 ± 27	207 ± 25
Spinal cord	301 ± 12	61 ± 6	252 ± 6
Forebrain	1693 ± 26	270 ± 9	349 ± 3
Striatum (frozen)	1293 ± 56	1263 ± 33	369 ± 8

previously reported (15), this phenomenon was magnified in the absence of magnesium ions. The NECA-displaceable nonspecific binding had a low affinity for NECA, with 50% displacement occurring between 1 μM and 10 μM NECA. None of the other adenosine agonists and antagonists tested were capable of displacing the low affinity component of [^{3}H]NECA binding (Table 4), indicating that the site is not an adenosine receptor.

Discussion

The site labeled by [^{3}H]NECA in the presence of 50 nM CPA is clearly an adenosine receptor, since adenosine agonists and antagonists of widely varied structure inhibit binding with affinities consonant with their known potencies at adenosine receptors. The evidence that this site is an A_2 receptor rests upon the ability of compounds with known A_1/A_2 selectivity in pharmacodynamic studies to show corresponding selectivity in inhibiting binding of [^{3}H]NECA relative to [^{3}H]CHA. Although detailed comparisons between binding selectivity and pharmacodynamic selectivity in the cardiovascular (33) and nervous (34) systems will be presented elsewhere, considerable published data pertinent to this subject are available. This literature strongly supports the A_2 nature of the [^{3}H]NECA-binding site. One of the most well characterized systems is the heart, where A_1 agonists cause decreases in heart rate and force (35), while A_2 agonists cause increases in coronary blood flow (36). The rank order of potency for coronary vasodilation in the dog (36) is identical to that for inhibition of [^{3}H]NECA binding in the presence of 50 nM CPA: NECA ≫ 2-chloroadenosine > *R*-PIA > CHA > *S*-PIA. Essentially the same rank order has been reported for numerous other A_2 responses, including relaxation of bovine coronary arteries (37), relaxation of cat cerebral arteries (38), relaxation of guinea pig aorta (39), and stimulation of adenylate cyclase in several tissues (2, 40) including rat cerebral microvessels (41). The methyl homolog of NECA is about twice as A_2-selective as NECA itself in the present study, in agreement with adenylate cyclase results in human platelets (42). Conversely, CHA and *R*-PIA, which are known to be highly A_1-selective in heart (33, 43), have a much higher affinity in [^{3}H]CHA binding than in [^{3}H]NECA binding. The rank order for adenosine agonists in decreasing rate and contractility in guinea pig heart (35) (*R*-PIA ≥ CHA ≥ NECA ≥ 2-chloroadenosine > *S*-PIA) agrees with the rank order for [^{3}H]CHA binding but differs from the rank order for [^{3}H]NECA binding. Additional evidence for the A_2 identity of the [^{3}H]NECA binding site is provided by CV-1808. CV-1808 and other adenosine analogs with bulky 2-position groups are potent stimulators of coronary blood flow, with no negative inotropic or chronotropic effects (44, 45). In agreement with this, CV-1808 is a potent inhibitor of [^{3}H]NECA binding and is the most A_2-selective of the compounds tested in the present study. CV-1808 previously has been shown to be about 50-fold less potent than 2-chloroadenosine in [^{3}H]CHA binding and in the A_1 receptor-mediated inhibition of neurogenic twitch in the rat vas deferens

TABLE 3

Organ distribution of different components of [^{3}H]NECA binding

Organs were dissected from male, 200-g Long-Evans rats and processed as described for striatum. Incubations were exactly as described in Experimental Procedures for striatum except that 10 mg of tissue were used (5 mg for heart and skeletal muscle) and 50 nM CPA was omitted. Values are means ± SE for triplicate incubations. This experiment was repeated two additional times with essentially identical results.

Organ	[^{3}H]NECA binding (cpm ± SE)				
	No addition	50 nM CPA	100 μM CPA	1 mM Theophylline	100 μM NECA
Striatum	5398 ± 88	2712 ± 41	432 ± 16	536 ± 15	215 ± 18
Whole brain	4854 ± 36	947 ± 28	399 ± 10	555 ± 8	233 ± 11
Testes	1033 ± 17	255 ± 3	190 ± 7	152 ± 9	85 ± 6
Liver	567 ± 17	596 ± 5	515 ± 11	296 ± 5	107 ± 13
Spleen	551 ± 7	436 ± 8	315 ± 4	223 ± 4	124 ± 5
Lung	317 ± 19	263 ± 20	251 ± 24	261 ± 34	186 ± 12
Kidney	217 ± 10	213 ± 13	178 ± 5	138 ± 2	78 ± 3
Thymus	190 ± 10	186 ± 11	144 ± 6	128 ± 13	89 ± 14
Adrenal	181 ± 31	172 ± 4	151 ± 15	106 ± 6	88 ± 2
Large intestine	161 ± 12	142 ± 10	111 ± 3	91 ± 4	69 ± 3
Heart	148 ± 8	114 ± 2	103 ± 4	99 ± 7	92 ± 3
Stomach	103 ± 20	95 ± 14	113 ± 23	84 ± 9	63 ± 5
Small intestine	102 ± 10	82 ± 5	61 ± 2	71 ± 6	70 ± 15
Skeletal muscle	98 ± 16	81 ± 2	80 ± 5	75 ± 3	65 ± 1
No tissue	96 ± 19	102 ± 10	86 ± 8	72 ± 5	85 ± 5

TABLE 4

Effects of NECA and other adenosine-related compounds on the low affinity component of [^{3}H]NECA binding to rat striatal membranes

All incubations (performed as described in Experimental Procedures) contained 50 nM CPA. The experiment was performed three times with essentially identical results.

Addition	[^{3}H]NECA Binding (cpm ± SE)	
	With 10 mM $MgCl_2$	Without $MgCl_2$
None	1705 ± 16	1381 ± 13
100 μM CPA	348 ± 10	592 ± 14
100 μM 2-Chloroado[a]	286 ± 13	502 ± 27
100 μM N^6-Benzylado	344 ± 16	599 ± 24
1 mM Theophylline	363 ± 20	551 ± 15
10 μM PD 113,297	371 ± 8	559 ± 21
1 μM NECA	364 ± 12	525 ± 28
10 μM NECA	226 ± 15	308 ± 5
100 μM NECA	196 ± 11	278 ± 13

[a] ado, adenosine.

(46). It also appears to be a potent inhibitor of adenosine uptake (46).

Adenosine A_1 receptors have been reported to exist in three interconvertible states which differ in their affinity for agonists, with affinity constants for CHA of 1.8, 15, and 430 nM (22). The state with the lowest affinity for CHA has a 5-fold higher affinity for DPX than the other two states. This raises the possibility that the site labeled by [^{3}H]NECA in the presence of 50 nM CPA in rat striatum may be a coupling state of the A_1 receptor with low affinity for agonists and high affinity for antagonists. This possibility can clearly be dismissed, however, since the antagonist CPT has 130-fold higher affinity in [^{3}H]CHA binding than in [^{3}H]NECA binding.

Several groups have observed differences among A_2 receptors in their regional distributions and affinities for adenosine (5,6). On the basis of these observations, Daly *et al.* (4) proposed that brain A_2 receptors be further subdivided into two subclasses: a receptor with a high affinity for adenosine (0.1–1 μM) which is localized mainly to striatum and which stimulates adenylate cyclase in broken cell preparations, and a receptor with a low affinity for adenosine (about 10 μM) which exists throughout the brain and which stimulates cyclic AMP accumulation in brain slices but apparently does not stimulate broken cell adenylate cyclase (at least in brain). By these criteria, the site labeled by [^{3}H]NECA in the presence of 50 nM CPA clearly belongs to the high affinity subclass of A_2 receptor.

To delineate further the differences between the high and low affinity A_2 receptors, it would be useful to compare the binding SAR in the present paper with the SAR for the low affinity A_2 receptor. A considerable amount of SAR information is available for the A_2 response in the VA13 human fibroblast cell line, a system in which adenosine causes a 100-fold increase in cyclic AMP with an EC_{50} of about 15 μM (18, 28, 47). The micromolar EC_{50} for adenosine in VA13 cells implies that the adenosine receptor in this preparation is a low affinity A_2 receptor, although it is not clear whether it is identical to the brain slice A_2 receptor described by Daly's group (4). In this regard, it should be noted that the low affinity adenosine receptor in human fibroblasts differs from the low affinity receptor in brain in being capable of stimulating cyclic AMP production in both intact and broken cells (47).

In Table 5, affinities of adenosine agonists and antagonists in [^{3}H]NECA binding to the high affinity A_2 receptor in rat striatum are compared with their affinities for mimicking or blocking the response to adenosine at the low affinity A_2 receptor in human fibroblasts. This information can be used to address the question of whether high and low affinity subclasses of A_2 receptors are distinct molecular entities, or whether they are simply interconvertible coupling states of the same receptor. Indeed, it is obvious from a comparison of the affinities of agonists and antagonists in the two systems (Table 5) that the [^{3}H]NECA binding site is agonist-preferring, whereas the A_2 receptor in human fibroblasts exhibits a marked preference for antagonists. However, several lines of evidence indicate that the two receptors are distinct proteins. CV-1674 has an affinity of 600 nM at the high affinity A_2 receptor but has been reported to be completely inactive at 1 mM in human fibroblasts (28). In order to confirm the lack of activity at the low affinity A_2 receptor of adenosine analogs with bulky 2-substituents, CV-1674 and CV-1808 were tested in VA13 human fibroblasts (28) at concentrations up to 1 mM.[5] The response to 1 mM CV-1674 was less than 4% of the maximal response to adenosine, and CV-1674 did not block the response to adenosine. From these results, it is apparent that the ED_{50} value for CV-1674 is considerably above 1 mM, implying that it possesses roughly 10,000-fold selectivity for the high affinity A_2 receptor over the low affinity A_2 receptor. CV-1808 was more active than CV-1674 in the human fibroblasts but, nevertheless, was at least 1000 times less active in this system than in [^{3}H]NECA binding. It is unlikely that a difference in affinity of this magnitude could be caused by differences in coupling state, especially since other agonists are as little as 11-fold selective for the high affinity subclass of A_2 receptor. Similarly, within the N^6-alkyladenosine series, N^6-methyladenosine and *R*-PIA have the same affinity at the low affinity fibroblast receptor, yet they differ by a factor of 30 in their affinities in [^{3}H]NECA binding. Additionally, some of the antagonists show as much as 20-fold preference for the low affinity A_2 receptor (Table 5). It is doubtful that a change in coupling state could account for a shift in affinity for antagonists of this magnitude. Preliminary studies on [^{3}H]NECA binding in human striatum indicate that these differences are not due to the use of rat tissue for [^{3}H]NECA binding (data not shown). Finally, the distinctly different regional distributions for the two receptors creates a presumption that they are under separate genetic control.

Since the high and low affinity types of A_2 receptor do appear to be distinct molecules, we propose that the high affinity A_2 receptor be designated A_{2a} and the low affinity receptor be designated A_{2b}. This nomenclature would appear to be mnemonically apt, since the affinities for most agonists would follow alphanumeric order, i.e., $A_1 > A_{2a} > A_{2b}$. This is illustrated most distinctly by CHA and *R*-PIA, which have affinities of roughly 1–10 nM at A_1 receptors, 100–1,000 nM at A_{2a} receptors, and 100,000–1,000,000 nM at A_{2b} receptors (see Tables 1 and 5). The A_{2a}/A_{2b} nomenclature should also help to avoid semantic confusion between the A_{2b} receptor and the low affinity coupling state of the A_{2a} receptor.

A_1 and A_2 receptors have been reported to differ in their stereoselectivity with respect to the isomers of PIA, with the A_1 receptor having a 40- to 100-fold preference for the *R* over the *S* diastereomer, and the (low affinity) A_2 receptor exhibiting only a 5-fold preference for the *R*-isomer (48). The *R*-PIA/*S*-

[5] R. F. Bruns and G. H. Lu, unpublished observations.

TABLE 5

Comparison of K_i values in [^{3}H]NECA binding (A_{2a}) with K_i and EC_{50} values in human fibroblast cyclic AMP accumulation (A_{2b})

Affinities of compounds as agonists or antagonists at adenosine receptors in human fibroblasts are taken from Refs. 7, 18, and 28. Full agonists are defined as compounds from the "full agonist" and "high efficacy partial agonist" categories in Ref. 28; the "high efficacy partial agonists" appear to actually be full agonists which do not reach the maximal response achieved by adenosine due to insolubility or P site inhibition (28). Nucleoside antagonists and partial agonists are from the "low efficacy partial agonist" and "competitive inhibitor" categories (28); when both the EC_{50} and K_i values were available for a partial agonist, the arithmetic mean of the two values was used.

Compound	A_{2a} K_i	A_{2b} K_i or EC_{50}	K_i ratio (A_{2b}/A_{2a})
	nM	nM	
Nucleoside Full Agonists			
1,N^6-Etheno-2-oxoado[a]	48,200	530,000	11.0
6-[(2-Hydroxy-5-nitrobenzyl)thio]inosine	34,700	>1,000,000	>28.8
N^6-Methylado	4,550	190,000	41.7
N^6-(2-Hydroxyethyl)ado	2,410	120,000	49.7
N^6-Phenylado	663	44,000	66.3
Ado-5′-carboxamide	120	24,000	200
Ado-5′-cyclopropylcarboxamide	13.4	3,000	223
Ado-5′-cyclohexylcarboxamide	4,300	>1,000,000	>233
Ado-5′-ethylcarboxamide (NECA)	10.3	2,600	253
Ado-5′-(2-hydroxyethyl)carboxamide	57.5	17,000	296
2-Oxoado (isoguanosine)	331	98,000	296
N^6-Cyclohexylado (CHA)	514	160,000	311
N^6-Benzylado	285	90,000	316
2-Chloroado	63.2	20,000	316
N^6-[(S)-1-Methyl-2-phenylethyl]ado (*S*-PIA)	1,820	750,000	413
Ado-5′-methylcarboxamide	66.8	33,000	494
N^6-[(*R*)-1-methyl-2-phenylethyl]ado (*R*-PIA)	124	150,000	1,210
2-(4-Methoxyphenyl)ado (CV-1674)	605	>1,000,000	>1,650
Nucleoside Antagonists and Partial Agonists			
5′-*O*-Acetylado	4,510	21,000	4.65
5′-Methylthioado	1,100	8,200	7.44
2-Chloro-5′-methylthioado	1,880	15,000	7.96
5′-Deoxy-5′-iodoado	637	6,800	10.7
Ado-5′-ethylcarboxylate	387	8,100	20.9
5′-*O*-Nitroado	335	9,000	26.8
Non-nucleoside Antagonists			
1,3-Diethyl-8-phenylxanthine (DPX)	863	40	0.0463
1,3-Diethylxanthine	22,200	1,200	0.0540
7-(2-Chloroethyl)theophylline	15,000	980	0.0653
1-Butyltheobromine	35,900	2,800	0.0780
8-(4-Sulfophenyl)theophylline	15,300	1,200	0.0786
8-(4-Nitrophenyl)theophylline	2,520	260	0.103
1-Ethyltheobromine	37,700	4,100	0.109
8-Propyltheophylline	10,000	1,300	0.130
1,3-Dipropylxanthine	5,160	680	0.132
1-Methylxanthine	36,200	6,600	0.183
8-(4-Chlorophenyl)theophylline	371	68	0.183
8-(4-Bromophenyl)theophylline	281	52	0.185
Theophylline (1,3-dimethylxanthine)	25,300	4,800	0.190
8-Phenyltheophylline	848	180	0.212
3-Isobutyl-1-methylxanthine	13,800	3,500	0.254
Caffeine (1,3,7-trimethylxanthine)	48,100	13,000	0.270
8-(4-Methoxyphenyl)theophylline	419	120	0.287
Alloxazine	2,720	1,100	0.405
8-Cyclopentyltheophylline (CPT)	1,440	710	0.492
Theobromine (3,7-dimethylxanthine)	187,000	130,000	0.695

[a] ado, adenosine.

PIA ratio at the high affinity A_2 receptor in the present paper is 15, indicating that the A_{2a} receptor is intermediate between the A_1 receptor and the A_{2b} receptor in its stereoselectivity for the isomers of PIA. The ratio of 15 in the present paper is in good agreement with the ratio of 10 reported for coronary blood flow in the dog (36). Since *R*-PIA/*S*-PIA ratios as low as 11 have been reported for A_1 receptors (12), this ratio is probably not a reliable criterion for subclassification of adenosine receptors.

A cyclopentyl group appears to confer optimal A_1 selectivity at both the N^6-position of adenosine and the 8-position of theophylline. This result may imply that the cyclopentyl moieties of CPT and CPA may bind to the same region on the receptor. Xanthines may therefore bind "backwards" compared to adenosine, with the five-membered ring of theophylline corresponding roughly in position to the six-membered ring of adenosine.

The affinity of adenosine in the A_1 and A_2 receptor binding assays could not be determined directly because of the necessity for adenosine deaminase in the incubation. However, it is possible to predict the affinity of adenosine indirectly if one assumes that changes at two nonadjacent positions in the adenosine structure will have additive effects on affinity.[6] This

[6] This is a type of Free-Wilson analysis; for a discussion of this method, see Ref. 49.

assumption has been shown to hold for the human fibroblast A_2 receptor (28). The three compounds 2-chloroadenosine, 5′-methylthioadenosine, and 2-chloro-5′-methylthioadenosine from the present paper (Table 1) provide one such prediction: if the 2-chloro modification has the same effect on adenosine that it has on 5′-methylthioadenosine, adenosine's A_1 affinity should be 12.8 nM [i.e., 9.33 × (281/206)] and its A_2 affinity should be 37.0 nM [i.e., 63.2 × (1100/1880)]. These estimated affinities are very close to the A_1 and A_2 affinities of 2-chloroadenosine (9.33 and 63.2 nM, respectively), confirming that 2-chloroadenosine is probably a good substitute for adenosine under conditions where breakdown of adenosine is a problem.

Results of the present study indicate that useful binding of [^{3}H]NECA to A_2 receptors can only be obtained in striatum, although detectable amounts of A_2 binding exist in other brain areas. The unusually restricted regional distribution of the A_2 receptor labeled by [^{3}H]NECA implies a specialized function for this receptor in the central nervous system. An involvement in exercise-induced motor fatigue would be consistent with the role of adenosine in oxygen supply/demand balance. Clinical conditions which might be related to the high affinity A_2 receptor include schizophrenia (34) and Parkinson's disease.

Our results and the results of others (15, 16, 19) with [^{3}H]NECA binding in peripheral tissue are not encouraging. Hüttemann *et al.* (15) reported that [^{3}H]NECA bound to low affinity sites in human platelets. Kinetics were extremely rapid, and binding could be inhibited about 50% by 10 mM $MgCl_2$. Although binding could be inhibited by 1 mM unlabeled NECA, 1 mM *R*-PIA had essentially no effect on binding, and the affinity of theophylline was 100-fold lower than its K_i for blocking the stimulation of cyclic AMP accumulation by NECA in human platelets (50). These results, which are inconsistent with binding to an adenosine receptor, emphasize the need for extreme caution in interpreting [^{3}H]NECA binding to peripheral tissues. Our results also emphasize the need for careful methodology to avoid misinterpretation of [^{3}H]NECA binding experiments. Several peripheral tissues had [^{3}H]NECA binding which could be blocked by unlabeled NECA and, in some tissues, by 1 mM theophylline, but not by 100 μM CPA. The ability of 10 mM $MgCl_2$ to lower nonspecific binding in the striatum is undoubtedly due to suppression of binding to this nonreceptor site; since 100 μM CPA was used to define nonspecific binding, binding to the nonreceptor site would be included in nonspecific binding. Yeung and Green (20) reported that a small amount of [^{3}H]NECA binding to rat striatal membranes could be blocked by unlabeled NECA but not by 100 μM *R*-PIA.

The results of the present study should facilitate the classification of A_2 responses in different tissues as A_{2a} or A_{2b}. The human platelet adenosine receptor, for instance, would appear to belong to the A_{2a} subclass, since aggregation is inhibited by nanomolar concentrations of NECA (50) and by low micromolar concentrations of adenosine analogs with bulky 2-substituents (51). It is of interest that, despite the ubiquity of the low affinity A_{2b} receptor, we are not aware of any report unequivocally linking this receptor to a pharmacodynamic response other than cyclic AMP generation.

Some of our results have implications for receptor binding methodology. Many studies use competition curves to divide multiple-receptor systems into their components when the labeled ligand is itself nonselective. We propose that, in order to demonstrate that two distinct, clearly separable sites have been identified, the two-site model should be shown to be statistically superior to a logistic (cooperative) model. This is a more rigorous criterion than proving that the two-site model is superior to a simple one-site model. It seems obvious that if a gradually sloping logistic curve can describe the data as accurately as a "stair-step" two-site curve, attempting to decompose the binding isotherm into two sites may lead to unreliable results. As shown in Fig. 2, a competitor needs at least a 500-fold selectivity for one site over the other before the two-site model provides a discernible improvement over the logistic curve.

Acknowledgments

We thank Dr. James Bristol for chemical support and helpful discussions, Dr. Walter Moos for providing CPA, Mr. James Fergus for A_1 K_i values, and Dr. Richard D. Green for providing a preprint of Ref. 20. We also acknowledge the numerous investigators who, by providing compounds, made this study possible.

References

1. van Calker, D., M. Müller, and B. Hamprecht. Adenosine regulates via two different types of receptors, the accumulation of cyclic AMP in cultured brain cells. *J. Neurochem.* **33**:999–1005 (1979).
2. Londos, C., D. M. F. Cooper and J. Wolff. Subclasses of external adenosine receptors. *Proc. Natl. Acad. Sci. USA* **77**:2551–2554 (1980).
3. Daly, J. W., R. F. Bruns, and S. H. Snyder. Adenosine receptors in the central nervous system: relationship to the central actions of methylxanthines. *Life Sci.* **28**:2083–2097 (1981).
4. Daly, J. W., P. Butts-Lamb, and W. Padgett. Subclasses of adenosine receptors in the central nervous system. Interaction with caffeine and related methylxanthines. *Cell. Mol. Neurobiol.* **1**:69–80 (1983).
5. Londos, C., J. Wolff, and D. M. F. Cooper. Adenosine receptors and adenylate cyclase interactions, in *Regulatory Function of Adenosine* (R. M. Berne, T. W. Rall, and R. Rubio, eds.). Martinus Nijhoff, Boston, 17–32 (1982).
6. Premont, J., M. Perez, G. Blanc, J.-P. Tassin, H.-M. Thierry, D. Herve, and J. Bockaert. Adenosine-sensitive adenylate cyclase in rat brain homogenates: kinetic characteristics, specificity, topographical, subcellular, and cellular distribution. *Mol. Pharmacol.* **16**:790–804 (1979).
7. Bruns, R. F., J. W. Daly, and S. H. Snyder. Adenosine receptors in brain membranes: binding of N^6-cyclohexyl[^{3}H]adenosine and 1,3-diethyl-8-[^{3}H]phenylxanthine. *Proc. Natl. Acad. Sci. USA* **77**:5547–5551 (1980).
8. Schwabe, U., and T. Trost. Characterization of adenosine receptors in rat brain by (−)[^{3}H]N^6-phenylisopropyladenosine. *Naunyn-Schmiedeberg's Arch. Pharmacol.* **313**:179–187 (1980).
9. Williams, M., and E. A. Risley, Biochemical characterization of putative central purinergic receptors by using 2-chloro[^{3}H]-adenosine, a stable analog of adenosine. *Proc. Natl. Acad. Sci. USA* **77**:6892–6896 (1980).
10. Wu. P. H., J. W. Phillis, K. Balls, and B. Rinaldi. Specific binding of 2-[^{3}H]chloroadenosine to rat brain cortical membranes. *Can. J. Physiol. Pharmacol.* **58**:576 (1980).
11. Murphy, K. M. M., and S. H. Snyder. Adenosine receptors in rat testes: labeling with ^{3}H-cyclohexyladenosine. *Life Sci.* **28**:917–920 (1981).
12. Trost, T., and U. Schwabe. Adenosine receptors in fat cells: identification by (−)-N^6-[^{3}H]phenylisopropyladenosine binding. *Mol. Pharmacol.* **19**:228–235 (1981).
13. Hosey, M. M., K. K. McMahon, and R. D. Green. Inhibitory adenosine receptors in the heart: characterization by ligand binding studies and effects on β-adrenergic receptor stimulated adenylate cyclase and membrane protein phosphorylation. *J. Mol. Cell. Cardiol.* **16**:931–942, 1984.
14. Fox, I. H., and L. Kurpis. Binding characteristics of an adenosine receptor in human placenta. *J. Biol. Chem.* **258**:6952–6955 (1983).
15. Hüttemann, E., D. Ukena, V. Lenschow, and U. Schwabe. R_a adenosine receptors in human platelets. Characterization by 5′-*N*-ethylcarboxamido[^{3}H]adenosine binding in relation to adenylate cyclase activity. *Naunyn-Schmiedeberg's Arch. Pharmacol.* **325**:226–233 (1984).
16. Schütz, W., E. Tuisl, and O. Kraupp. Adenosine receptor agonists: binding and adenylate cyclase stimulation in rat liver plasma membranes. *Naunyn-Schmiedeberg's Arch. Pharmacol.* **319**:34–39 (1982).
17. Bruns, R. F. Some adenosine antagonists and adenylate cyclase inhibitors. *Soc. Neurosci. Abstr.* **4**:442 (1978).
18. Bruns, R. F. Adenosine antagonism by purines, pteridines and benzopteridines in human fibroblasts. *Biochem. Pharmacol.* **30**:325–333 (1981).
19. Buckley, N., and G. Burnstock. Autoradiographic demonstration of peripheral adenosine binding sites using [^{3}H]NECA. *Brain Res.* **269**:374–377 (1983).
20. Yeung, S.-M. H., and R. D. Green. [^{3}H]5′-*N*-Ethylcarboxamide adenosine binds to both R_a and R_i adenosine receptors in rat striatum. *Naunyn-Schmiedeberg's Arch. Pharmacol.* **325**:218–225 (1984).
21. Bruns, R. F., G. H. Lu, and T. A. Pugsley, Binding of ^{3}H-NECA to a subtype of A_2 adenosine receptor in rat striatal membranes. *Soc. Neurosci. Abstr.* **10**:957 (1984).

22. Yeung, S.-M. H., and R. D. Green. Agonist and antagonist affinities for inhibitory adenosine receptors are reciprocally affected by 5′-guanylylimidodiphosphate or *N*-ethylmaleimide. *J. Biol. Chem.* **258**:2334–2339 (1983).
23. Bevington, P. R. *Data Reduction and Error Analysis for the Physical Sciences.* McGraw-Hill, New York, 200–202 (1969).
24. Korner, M., C. Gilon, and M. Schramm. Locking of hormone in the β-adrenergic receptor by attack on a sulfhydryl in an associated component. *J. Biol. Chem.* **257**:3389–3396 (1982).
25. Moos, W. H., D. S. Szotek, and R. F. Bruns. N^6-Cycloalkyladenosines. Potent, A_1-selective adenosine agonists. *J. Med. Chem.* **28**:1383–1384 (1985).
26. Agarwal, R. P., T. Spector, and R. E. Parks, Jr. Tight-binding inhibitors. IV. Inhibition of adenosine deaminases by various inhibitors. *Biochem. Pharmacol.* **26**:359–369 (1977).
27. Lohse, M. J., V. Lenschow, and U. Schwabe. Two affinity states of R_i adenosine receptors in brain membranes. Analysis of guanine nucleotide and temperature effects on radioligand binding. *Mol. Pharmacol.* **26**:1–9 (1984).
28. Bruns, R. F. Adenosine receptor activation in human fibroblasts: nucleoside agonists and antagonists. *Can. J. Physiol. Pharmacol.* **58**:673–691 (1980).
29. Bruns, R. F., J. W. Daly, and S. H. Snyder. Adenosine receptor binding: structure-activity analysis generates extremely potent xanthine antagonists. *Proc. Natl. Acad. Sci. USA* **80**:2077–2080 (1983).
30. Hamilton, H. H., D. F. Ortwine, D. F. Worth, E. W. Badger, J. A. Bristol, R. F. Bruns, S. J. Haleen, and R. P. Steffen. Synthesis of xanthines as adenosine antagonists, a practical quantitative structure activity relationship application. *J. Med. Chem.* **28**:1071–1079 (1985).
31. Psychoyos, S., C. J. Ford, and M. A. Phillipps. Inhibition by etazolate (SQ 20009) and cartazolate (SQ 65396) of adenosine-stimulated [^{3}H]cAMP formation in [2-^{3}H]adenine-prelabeled vesicles prepared from guinea pig cerebral cortex. *Biochem. Pharmacol.* **31**:1441–1442 (1982).
32. Ebersolt, C., J. Premont, A. Prochiantz, M. Perez, and J. Bockaert. Inhibition of brain adenylate cyclase by A_1 adenosine receptors: pharmacological characteristics and locations. *Brain Res.* **267**:123–129 (1983).
33. Mertz, T. E., R. F. Bruns, C. L. Germain, and D. B. Evans. Cardiovascular and receptor-binding selectivity of adenosine agonists in rats. *Pharmacologist* **26**:143 (1984).
34. Heffner, T. G., D. A. Downs, J. A. Bristol, R. F. Bruns, S. E. Harrigan, W. H. Moos, K. L. Sledge, and J. N. Wiley. Antipsychotic-like effects of adenosine receptor agonists. *Pharmacologist* **27**:293 (1985).
35. Evans, D. B., J. A. Schenden, and J. A. Bristol. Adenosine receptors mediating cardiac depression. *Life Sci.* **31**:2425–2432 (1982).
36. Kusachi, S., R. D. Thompson, and R. A. Olsson. Ligand selectivity of dog coronary adenosine receptor resembles that of adenylate cyclase stimulatory (R_a) receptors. *J. Pharmacol. Exp. Ther.* **227**:316–321 (1981).
37. Mustafa, S. J., and O. A. Abdallah. Evidence suggesting an R_a-type adenosine receptor in bovine coronary arteries. *J. Pharmacol. Exp. Ther.* **232**:49–56 (1984).
38. Edvinsson, L., and B. B. Fredholm. Characterization of adenosine receptors in isolated cerebral arteries of cat. *Br. J. Pharmacol.* **80**:631–637 (1983).
39. Collis, M. G., and C. M. Brown. Adenosine relaxes the aorta by interacting with an A_2 receptor and an intracellular site. *Eur. J. Pharmacol.* **96**:61–69 (1983).
40. Woodcock, E. A., R. Loxley, E. Leung, and C. I. Johnston. Demonstration of R_a-adenosine receptors in rat renal papillae. *Biochem. Biophys. Res. Commun.* **121**:434–440 (1984).
41. Schütz, W., G. Steurer, and E. Tuisl. Functional identification of adenylate cyclase-coupled adenosine receptors in rat brain microvessels. *Eur. J. Pharmacol.* **85**:177–184 (1982).
42. Ukena, D., E. Böhme, and U. Schwabe. Effects of several 5′-carboxamide derivatives of adenosine on adenosine receptors of human platelets and rat fat cells. *Naunyn-Schmiedeberg's Arch. Pharmacol.* **327**:36–42 (1984).
43. Haleen, S. J., and D. B. Evans. Selective effects of adenosine receptor agonists upon coronary resistance and heart rate in isolated working rabbit hearts. *Life Sci.* **36**:127–137 (1985).
44. Kawazoe, K., N. Matsumoto, M. Tanabe, S. Fujiwara, M. Yanagimoto, M. Hirata, and K. Kikuchi. Coronary and cardiohemodynamic effects of 2-phenylamino-adenosine (CV-1808) in anesthetized dogs and cats. *Arzneim. Forsch.* **30**:1083–1087 (1980).
45. Einstein, R., J. A. Angus, L. B. Cobbin, and M. H. Maguire. Separation of vasodilator and negative chronotropic actions in analogues of adenosine. *Eur. J. Pharmacol.* **19**:246–250 (1972).
46. Taylor, D. A., and M. Williams. Interaction of 2-phenylamino-adenosine (CV 1808) with adenosine systems in rat tissues. *Eur. J. Pharmacol.* **85**:335–338 (1982).
47. Clark, R. B., and M. N. Seney. Regulation of adenylate cyclase from cultured human cell lines by adenosine. *J. Biol. Chem.* **251**:4239–4246 (1976).
48. Smellie, F. W., J. W. Daly, T. V. Dunwiddie, and B. J. Hoffer. The dextro and levorotatory isomers of *N*-phenylisopropyladenosine: stereospecific effects on cyclic AMP-formation and evoked synaptic responses in brain slices. *Life Sci.* **25**:1739–1748 (1982).
49. Martin, Y. C. *Quantitative Drug Design, A Critical Introduction.* Marcel Dekker, New York, 329–347 (1978).
50. Cusack, N. J., and S. M. O. Hourani. 5′-*N*-Ethylcarboxyamido-adenosine: a potent inhibitor of human platelet aggregation. *Br. J. Pharmacol.* **72**:443–447 (1981).
51. Kikugawa, K., H. Suehiro, and M. Ichino. Platelet aggregation inhibitors. 6.2-Thioadenosine derivatives. *J. Med. Chem.* **16**:1381–1388 (1973).

Send reprint requests to: Dr. Robert F. Bruns, Department of Pharmacology, Warner-Lambert/Parke-Davis Pharmaceutical Research, Ann Arbor, MI 48105.